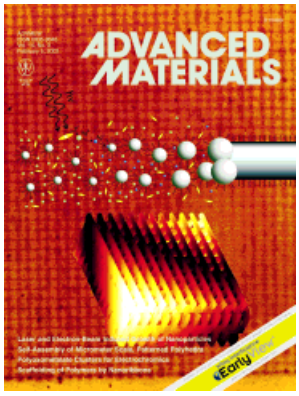

Cover: *Metallic nanostructures such as that displayed on the cover (bottom image and background) can be fabricated in nanoparticle-seeded polymer nanocomposites by either two-photon laser exposure (schematically illustrated on the cover) or electron-beam irradiation. Full details are to be found in the article by Perry, Marder and co-workers on page 194.*

ADVANCED MATERIALS

www.advmat.de

Communications

  0935-9648/02/0302-0175 $ 17.50+.50/0

ADVANCED MATERIALS

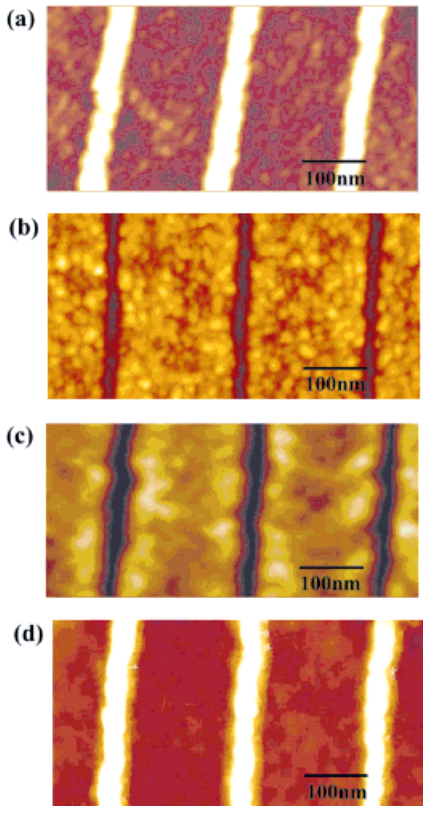

Fig. 5. a) AFM image of MoO_3 lines formed by AFM local oxidation of a Mo film on a 35 nm thick PMMA film on SiO_2. b) AFM image of gaps in the Mo film after dissolving the MoO_3 lines in (a) with H_2O. c) AFM image of the same area as in (b) after O_2 plasma etching. d) ~35 nm wide Ti lines formed after deposition of Ti on (c) and liftoff of the Mo/PMMA resist.

use of water as a chemical etchant makes the lithography process compatible with biological systems. SPL strategies for nanoscale patterning of biological molecules could be devised.

Received: September 7, 2001
Final version: October 31, 2001

[1] C. F. Quate, *Surf. Sci.* **1997**, *386*, 259.
[2] H. Dai, N. Franklin, J. Han, *Appl. Phys. Lett.* **1998**, *73*, 1508.
[3] E. B. Cooper, S. R. Manalis, H. Fang, H. Dai, K. Matsumoto, S. C. Minne, T. Hunt, C. F. Quate, *Appl. Phys. Lett.* **1999**, *29*, 3566.
[4] S. Minne, J. Adams, G. Yaralioglu, S. Manalis, A. Atalar, C. Quate, *Appl. Phys. Lett.* **1998**, *73*, 1742.
[5] J. A. Dagata, J. Schneir, H. H. Harary, C. J. Evans, M. T. Postek, J. Bennett, *Appl. Phys. Lett.* **1990**, *56*, 2001.
[6] E. Snow, P. Campbell, *Appl. Phys. Lett.* **1994**, *64*, 1932.
[7] K. Matsumoto, M. Ishii, K. Segawa, Y. Oka, B. J. Vartanian, J. S. Harris, *Appl. Phys. Lett.* **1996**, *68*, 34.
[8] E. Dubois, J. L. Bubendorff, *J. Appl. Phys.* **2000**, *87*, 8148.
[9] J. Servat, P. Gorostiza, F. Sanz, F. Perez-Murano, N. Barniol, G. Abadal, X. Aymerich, *J. Vac. Sci. Technol. A* **1997**, *14*, 1208.
[10] K. Wilder, C. F. Quate, D. Adderton, R. Bernstein, V. Elings, *Appl. Phys. Lett.* **1998**, *73*, 2527.
[11] D. C. Tully, K. Wilder, J. M. Frechet, A. Trimble, C. F. Quate, *Adv. Mater.* **1999**, *11*, 314.
[12] M. Lercel, G. Redinbo, H. G. Craighead, C. W. Sheen, D. L. Allara, *Appl. Phys. Lett.* **1994**, *65*, 974.
[13] G. Y. Liu, Y. L. Qian, *Acc. Chem. Res.* **2000**, *33*, 457.
[14] S. Hu, A. Hamidi, S. Altmeyer, T. Koster, B. Spangenberg, H. Kurz, *J. Vac. Sci. Technol. B* **1998**, *16*, 2822.
[15] R. Piner, J. Zhu, F. Xu, S. Hong, C. A. Mirkin, *Science* **1999**, *283*, 661.
[16] Y. Li, B. Maynor, J. Liu, *J. Am. Chem. Soc.* **2001**, *123*, 2105.
[17] H. Sugimura, T. Uchida, N. Kitamura, H. Masuhara, *J. Vac. Sci. Technol. B* **1994**, *12*, 2884.
[18] R. Held, T. Heinzel, P. Studerus, K. Ensslin, M. Holland, *Appl. Phys. Lett.* **1997**, *71*, 2689.
[19] H. Song, M. Rack, K. Abugharbieh, S. Lee, D. K. Ferry, S. R. Allee, *J. Vac. Sci. Technol. B* **1994**, *12*, 3720.
[20] D. W. Wang, L. M. Tsau, K. L. Wang, P. Chow, *Appl. Phys. Lett.* **1995**, *67*, 1295.

Laser and Electron-Beam Induced Growth of Nanoparticles for 2D and 3D Metal Patterning**

By *Francesco Stellacci*, *Christina A. Bauer*, *Timo Meyer-Friedrichsen*, *Wim Wenseleers*, *Valérie Alain*, *Stephen M. Kuebler*, *Stephanie J. K. Pond*, *Yadong Zhang*, *Seth R. Marder*,* and *Joseph W. Perry**

In recent years, advances in the patterning of polymers[1,2] and semiconductors[3] have enabled the fabrication of integrated micro- and nanosystems[4,5] with high levels of complexity and functionality. Further enhancements in the capabilities of these systems could be realized if versatile methods for the patterning of two-dimensional (2D) and three-dimensional (3D) metallic structures on the micro- and nanoscale were available. Progress has been made on the assembly of metal nanoparticles[6,7] for the fabrication of nanoscale structures,[8] and electron-beam patterning of nanoparticle monolayers has recently been demonstrated.[9] In this communication, we report on composite materials containing metal nanoparticles that, upon laser or electron-beam irradiation, lead to growth of nanoparticles into defined continuous metal patterns. Excitation by one- or two-photon absorption allowed for the one-step laser writing of continuous silver, copper, and gold metal microstructures in one-dimensional (1D), 2D, and 3D patterns. Electron-beam irradiation of ultrathin films of a dye-attached metal nanoparticle composite allowed for high-sensitivity writing of lines and pads, demonstrating the possibility of using such materials for direct electron-beam lithography of metal. This nanocomposite approach, based on photo-reductive or electron-beam induced growth of nanoparticles, provides a versatile new method for patterning metal features that could have an impact on electronic, optical, and electromechanical technologies.

Several methods for laser writing of metal features have been investigated previously including laser pyrolysis[10] of gas

[*] Dr. J. W. Perry, Dr. S. R. Marder, Dr. F. Stellacci, C. A. Bauer, Dr. T. Meyer-Friedrichsen, Dr. W. Wenseleers, Dr. V. Alain, Dr. S. M. Kuebler, S. J. K. Pond, Dr. Y. Zhang
Department of Chemistry, The University of Arizona
1306 E. University Blvd., Tucson, AZ 85721 (USA)
E-mail: jwperry@u.arizona.edu, smarder@u.arizona.edu

[**] The authors thank Philip Anderson for TEM measurements, Gary Chandler for SEM imaging, Paul Clem and David Mathine for conductivity measurements, and Ken Nebesny for XPS measurements. Support of this work by the Office of Naval Research and the National Science Foundation is gratefully acknowledged. TMF acknowledges the German Science Foundation (DFG) for financial support.

  0935-9648/02/0302-0194 $ 17.50+.50/0

phase precursors or metal complexes in a polymer matrix, and photoreduction of metal salts in a sol–gel matrix[11] or photographic film.[12] While continuous metal features have been produced by pyrolysis, the conditions were rather harsh and the methods were limited to substrates and surface features that could withstand high temperatures and high-power laser exposure. Pyrolysis of films of ligand coated metal nanoparticles has recently been shown to give rise to very thin metal films.[13] Photoreduction of metal salts is a potentially more versatile approach since it can be performed at ambient temperature with relatively low power. However, experiments to date using photoreduction in a matrix[11,12] have resulted only in patterns of isolated metal particles and subsequent development steps (such as electroless deposition)[14] were needed to form continuous metal, thereby complicating the process and limiting the spatial resolution.

We sought to develop materials for the one-step photoreductive writing of continuous metal features in a matrix or on a surface. A basic scheme for photoreduction[15] of metal ions by a dye sensitizer is shown in Figure 1. Transfer of an electron from the excited dye to the metal ion leads to formation of a silver atom which can either: 1) react with other silver atoms to nucleate, 2) add onto an existing particle, or 3) undergo charge recombination. Thus, the formation and growth of metal particles is limited by the competition between the rate of growth or nucleation and charge recombination, as well as local depletion of metal ions. Since growth rates are in general much larger than nucleation rates and depend on the number of nucleation centers, we reasoned that introduction of nanoparticle seeds into the composite could significantly enhance the efficiency of formation of a continuous metal phase. To this end, we explored the incorporation of ligand-coated metal nanoparticles into a photoactive material system to provide controllable nucleation centers.

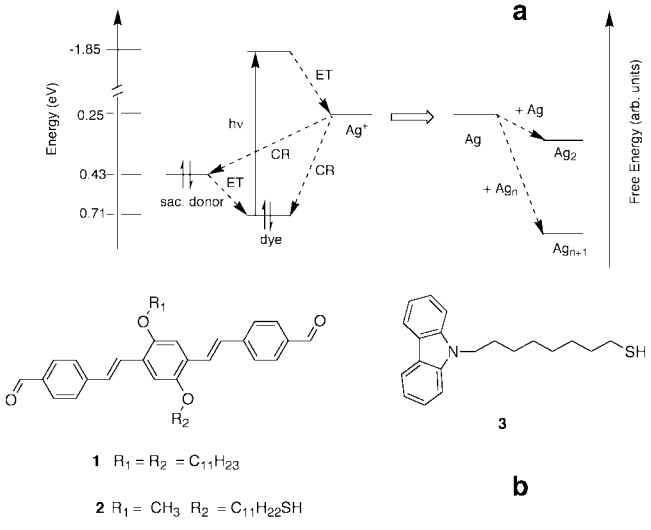

Fig. 1. a) Schematic illustration of a three-state photoinduced electron-transfer model for photoreduction of silver ions and growth of silver nanoparticles. Left: A schematic frontier orbital energy level diagram illustrating one-photon excitation of a sensitizing dye, electron transfer (ET) from the excited dye to Ag^+, ET from the sacrificial donor to the highest occupied molecular orbital (HOMO) level of the dye, and charge recombination (CR) from reduced Ag^+ to the dye and to the sacrificial donor. ET from the sacrificial donor to the dye HOMO level regenerates the neutral form of the dye, allowing further absorption of photons and generation of silver atoms. The approximate energies of the levels were derived from electrochemical measurements against the ferrocenium/ferrocene couple. Right: Qualitative free energy diagram illustrating the reaction of photogenerated silver atoms with nanoparticle seeds that act as a thermodynamic sink, allowing fast growth of nanoparticles relative to nucleation. b) Structures of the dye (**1**) and ligands (**2** and **3**) used in this study. The syntheses of these compounds will be reported separately. The synthesis of the mixed-ligand-coated nanoparticles was performed using a modification of the one-phase method of ref. [27] and the dye-attached nanoparticles were prepared following the method of ref. [28].

We designed and formulated a polymer nanocomposite material for direct writing of silver metal based on the photoreductive growth of nanoparticles. The components of the nanocomposite were: 1) an organic-solvent-soluble silver salt ($AgBF_4$) as a precursor to metal atoms, 2) a suitable photoreducing dye as sensitizer, 3) ligand-coated silver nanoparticles as seeds, and 4) polyvinylcarbazole (PVK) as a host polymer and sacrificial reducing agent, (see Fig. 1). The choice of the dye was critical to achieving: 1) negligible thermal reduction of silver ions, 2) efficient one- or two-photon excitation, and 3) efficient reduction of silver ions from the excited singlet state. These characteristics were achieved using a bis-electron-acceptor substituted π-conjugated organic chromophore,[16] whose structure and energy levels are shown in Figure 1. The dye **1** has an excited state lifetime of 1.79 ns, which is sufficiently long to facilitate electron transfer (ET), and a significant peak two-photon absorption cross-section of 360×10^{-50} $cm^4\,s\,photon^{-1}$ at 700 nm, referenced against a coumarin 307 standard.[17]

To achieve homogeneous dispersion of the nanoparticles and high optical quality films, the particles should be soluble, to afford processability and compatibility with the matrix, and stable relative to spontaneous aggregation. Although alkylthiol-coated metal nanoparticles are reasonably stable[18] and soluble,[19] their solubility in polymer matrices is rather limited due to the formation of ordered aggregates[20] as a result of interdigitation[21] of the ligands. To overcome this limitation, we prepared metal nanoparticles coated with a mixture of alkylthiol ligands of different lengths, to disrupt the interdigitation, and alkylthiols functionalized at the chain end with a compatibilizing carbazole group, **3**. The enthalpy of the de-interdigitation transition[22] for these particles was reduced by four times compared to simple octylthiol-coated particles (from 21 to 6 J/mol of ligand), leading to greatly improved solubility and homogeneity of the composites.

To establish the role of each component in the metal writing process, films with various compositions were subjected to continuous wave (CW) laser exposures with a range of intensities (0.45 to 4×10^5 W/cm^2). In films initially free of nanoparticles, laser excitation over the full range of intensity led only to the formation of relatively small, well-separated nanoparticles with a broad size distribution, as evidenced by optical absorption spectroscopy and transmission electron microscopy (TEM, Fig. 2). In films with added nanoparticles, we observed an increase in the size of the incorporated particles at low exposure levels (see Fig. 2). In separate experiments using single-shot pulsed laser exposures (0.1 J/cm^2; 532 nm,

  0935-9648/02/0302-0195 $ 17.50+.50/0

ADVANCED MATERIALS

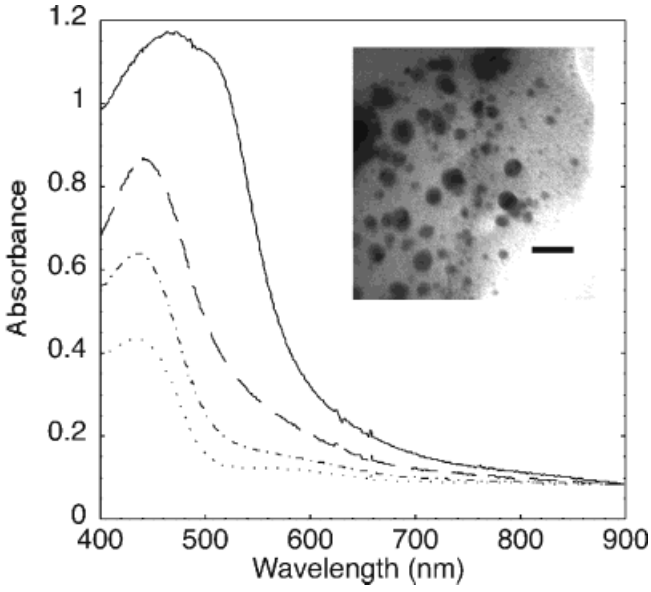

Fig. 2. Optical absorption spectroscopy evidence for accelerated photoinduced growth of nanoparticles in seeded nanocomposites. Dotted line: spectrum of a composite without nanoparticle seeds (film A, see Experimental), showing the absorption band at ~435 nm due to dye **1** [29]. Dot-dashed line: spectrum of film A after a 30 min CW-laser irradiation at 514.5 nm with an intensity of 0.45 W/cm^2 shows an increased absorption at 426 nm, indicating formation of isolated nanoparticles. Dashed line: spectrum of a composite with 0.5 wt.-% nanoparticle seeds (film B). Solid line: spectrum of film B following identical irradiation to that for film A. The large increase in the width of the band indicates a substantial increase in the mean radius [30] of the nanoparticles, consistent with the TEM results discussed in the text. The inset shows a TEM image of the nanoparticles formed in a 100 nm thick film, with the same composition as film A, following irradiation overnight at 419 nm in a photochemical reactor (scale bar 33 nm).

8 ns), TEM measurements showed that the particle radius increased from 3.0 ± 0.3 nm to 5.0 ± 0.3 nm, with no apparent increase in the particle number density. In contrast to the results for films with no added nanoparticles, we observed the formation of continuous metal patterns under higher levels of CW laser exposure. These results demonstrate that photoactivated growth of metal nanoparticles can lead to continuous metal in a solid matrix. Further studies revealed that composites without dye or metal salt are inactive relative to the formation of continuous metal up to the highest levels of exposure, consistent with the growth of the metal nanoparticles being driven by the dye-sensitized photoreduction of silver ions. Lastly, addition of ethyl carbazole (30 wt.-%) as a plasticizer led to a 40 % reduction in the intensity threshold for writing metal, consistent with a significant role of mass transport in the growth process. The necessity of the key components (nanoparticles, salt, and dye) for photogeneration of metal was established with experiments performed under both one- (488 and 514.5 nm) and two-photon (730 and 800 nm) excitation.

In our nanocomposite films, continuous patterns of silver metal could be written using two-photon excitation. An example illustrating the fabrication of a 3D metallic microstructure using two-photon excitation is shown in Figures 3a–d. A 100 μm thick film was exposed to a 3D pattern, illustrated in Figure 3a, using a tightly focused laser beam of 120 fs pulses

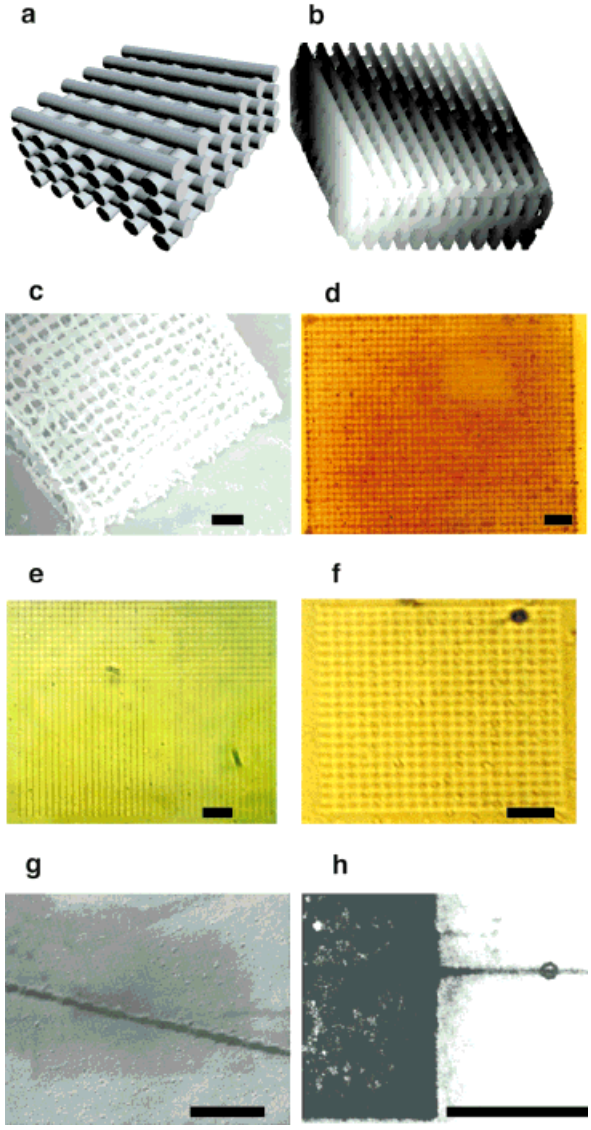

Fig. 3. Metallic structures fabricated in nanocomposites by two-photon scanning laser exposure and electron-beam irradiation. a) Model of a target 3D structure: a "stack-of-logs" type structure. b) Image of the actual 3D silver structure fabricated in a nanoparticle-seeded polymer nanocomposite by two-photon laser exposure; the image was reconstructed from a series of two-photon fluorescence microscopy images obtained at varying depths in the sample. c) SEM image of the free-standing 3D silver structure in (b) after removal of unexposed material using dichloromethane. d) Transmission optical microscopy (TOM) image of the silver microstructure in the polymer nanocomposite after two-photon laser exposure. The film was formed by dissolving 220 mg of PVK, 110 mg of *N*-ethylcarbazole, 11 mg of dye **1**, 2 mg of mixed ligand nanoparticles, and 24 mg of $AgBF_4$ in 2 mL of degassed $CHCl_3$. e) TOM image of copper microstructure in a different polymer nanocomposite fabricated by two-photon laser exposure. The film was formed by dissolving 66 mg of poly(methylmethacrylate) PMMA, 1.1 mg of ligand coated copper nanoparticles, 5 mg of $CuP(CH_3)_3I$, and 3 mg of dye **1** in 0.6 mL of degassed $CHCl_3$ and casting under an argon atmosphere. f) TOM image of a gold microstructure fabricated by two-photon laser exposure. The film was formed by dissolving 66 mg of PMMA, 1.1 mg of ligand-coated gold nanoparticles, 5 mg of $AuP(CH_3)_3Br$, and 3 mg of dye **1** in 0.6 mL of $CHCl_3$ and casting as above. g) SEM image of a silver line fabricated on an indium-tin oxide coated substrate by using two-photon laser exposure. h) SEM image of a silver pad and line fabricated by electron-beam lithographic exposure of a nanocomposite comprised of 95 wt.-% dye-attached ligand-coated silver nanoparticles and 5 % $AgBF_4$. Films of this composite with a thickness of ~20 nm were formed by evaporation of a $CHCl_3$ solution of nanoparticles and salt on an ITO coated substrate. Scale bars for the TOM images: 25 μm, scale bars for the SEM images: 10 μm.

  0935-9648/02/0302-0196 $ 17.50+.50/0

at 730 nm with an average power of 15 mW at a scan rate of 25 μm/s. In the two-photon excitation process, the absorption of light energy is confined to the focal volume,[23] hence the photoreduction of metal ions is localized to a volume of ~0.1 μm^3. Scanning the position of the focus in the material under computer control allows patterned exposure of the nanocomposite resulting in the formation of 3D microstructures.[24,25] Optical transmission and two-photon fluorescence microscopy show that the optical quality of the film is good and the 3D microstructure is formed with high fidelity. Removal of the polymer resulted in a free-standing, albeit somewhat deformed, metal microstructure that we imaged using scanning electron microscopy (SEM). X-ray photoelectron spectroscopy (XPS) of a series of lines patterned in a similar manner established that the lines were primarily silver metal (Ag^0). Initial electrical measurements on laser written silver lines, both within the composite and after removal of the polymer, showed them to be conductive, with a resistivity of $\rho \approx 10^{-3}$ Ω cm (as compared to 1.6×10^{-6} Ω cm for bulk silver), however the contribution of contact impedance has not yet been separated. Using analogous nanocomposites to that used for silver, we were able to write patterns of copper and gold, (Figs. 3e and f) thus demonstrating the utility of the approach for patterning of noble metals.

One-photon excitation of the nanocomposite can be used for the writing of 1D and 2D metal patterns and optical data storage. We have fabricated metal lines with a width as small as 500 nm, as well as larger pads, using tightly-focused, CW 514.5 nm laser excitation. The reflectivity of laser-written silver pads was determined to be 0.25, which is six times higher than that of the nanocomposite itself. The intensity threshold for writing metal using one-photon excitation is 4×10^5 W/cm^2 at 25 μm/s; indicating that a laser power of ≈1 mW, which is readily available from commercial lasers, is sufficient for recording. This threshold is set by the exposure level needed to generate a sufficient number of silver atoms to produce a reflective metal phase. It should be emphasized that the films are photochemically stable and photoactive after months of storage without special precautions. These results suggest the possible use of these nanocomposites as an optical data storage medium.

Since ligand-coated nanoparticles can self organize into ordered monolayer films,[6] we investigated whether the laser-driven metal nanoparticle growth approach to patterning could be realized in such ultrathin films. To ensure a high local concentration of dye at the surface of the nanoparticle and to minimize heterogeneity, ligand-coated nanoparticles, in which a small fraction of the ligands was functionalized with a pendant dye, **2**, were prepared. Laser exposure of a sparse submonolayer film (chosen to facilitate imaging), comprised of dye-attached nanoparticles and a metal salt as dopant, induced growth of the nanoparticles (Fig. 4a,b), as in the polymer nanocomposite discussed above. On the other hand, a film based on particles without dye showed no growth upon exposure. Since the optical absorption was dominated by the nanoparticles in both types of films, the thermal loading was identical for both. Therefore, we rule out thermally induced growth mechanisms. Scanning laser beam exposure of films (~20 nm thickness) led to the direct formation of metal patterns that could be isolated by removal of unexposed material using dichloromethane.

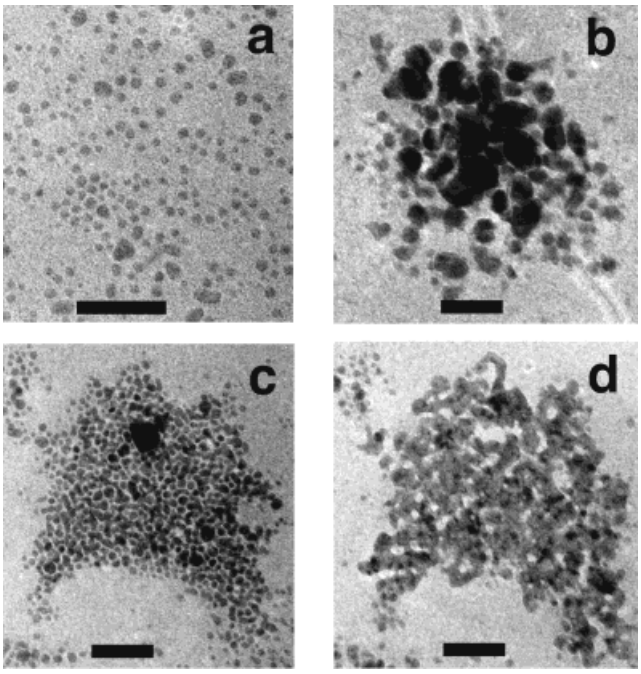

Fig. 4. Laser and electron-beam induced growth of silver nanoparticles in a nanoparticle/salt composite. a) TEM image of a composite prior to laser exposure, showing a domain of ordered nanoparticles with a mean radius of 6 nm. b) Image of composite following one-photon excitation at 488 nm for 240 min with an intensity of 1.5 W/cm^2 (to ensure depletion of the silver salt), showing growth of particles. c) Image of composite prior to electron-beam irradiation, showing a domain of ordered nanoparticles with the same mean radius as in (a). d) Image of composite following electron-beam irradiation in the TEM instrument for 15 min showing growth of particles and formation of a nearly consolidated metal domain. Scale bars: 50 nm.

It has been shown that ultrathin nanoparticle films can be used to pattern metals by electron-beam irradiation.[26] We investigated electron-beam exposure of films of dye-attached nanoparticle/salt composites in a TEM instrument. Such exposures induced growth of the metal particles as shown in Figures 4c,d. Experiments were performed with the same level of exposure on films of nanoparticles lacking the dye-functionalized ligand, and in this case nanoparticle growth was not observed, indicating that electron impact ionization or reduction of the dye is important in the process. Direct writing of metal patterns was achieved by scanning electron-beam exposure in a SEM instrument. Dissolution of unexposed material led to the isolation of the written lines and pads on the substrate, with feature sizes as small as 300 nm, as shown in Figure 3h. A unique and potentially useful feature of these nanocomposites is that the same films are electron-beam and photochemically active; thus, there is potential for use of both patterning techniques on the same film.

In conclusion, we have shown that polymer nanocomposites containing metal nanoparticles, a silver salt, and an appropriate photoreducing dye are efficient precursors for direct laser

  0935-9648/02/0302-0197 $ 17.50+.50/0

ADVANCED MATERIALS

writing of continuous metal structures. Truly 3D free-standing metallic structures with a height of 100 μm have been microfabricated and characterized. Photoactive nanocomposites have been formed using nanoparticles with covalently attached photoreducing dye molecules. These nanocomposites are active to both photon and electron-beam stimuli and yield continuous metallic structures. We believe that optical or electron-beam induced growth of nanoparticles provides a versatile new approach to the patterning of metal from the micrometer to the nanometer length scales in 2D and 3D. This approach may have applications in the fabrication of new types of structures, interconnects, and components in electronic, optical, and electromechanical devices.

Experimental

Chemicals were purchased from Aldrich and used as received unless specified. Spectrophotometric grade solvents were used for film processing.

Films were prepared by solvent evaporation under an inert atmosphere (Ar) saturated by the solvent vapor. Microscope glass slides (75 × 25 mm^2) were cleaned by sonication in water, ethanol, and acetone and then rinsed with isopropanol.

Film A was formed by dissolving 60 mg of PVK, 30 mg of *N*-ethylcarbazole, 3 mg of dye **1**, and 6 mg of $AgBF_4$ in 2 mL of $CHCl_3$. Film B was prepared similarly with the addition of 0.3 mg of mixed-ligand metal nanoparticles (mean diameter of 5 ± 1 nm), bearing 1-octylthiol and ligand **3** in a 3:1 ratio.

Two-photon writing experiments were performed using a femtosecond mode-locked Ti:sapphire laser (Spectra Physics, Tsunami) pumped by a diode-pumped YVO_4 laser (Spectra Physics, Millennia). The average pulse length of the laser was 120 fs, and the repetition rate was 82 MHz. Unless specified otherwise the wavelength used was 760 nm. One-photon writing experiments were perfomed using an Ar^+ ion laser (Spectra Physics, 2020).

The film samples were mounted on a micropositioner (Sutter MP-285). The laser beam was focused on the sample using an inverted microscope (Nikon Eclipse TE300). A computer controlled both the micropositioner and a shutter (Newport 846HP). The combination of the micropositioner movements and the opening/closing of the shutter were synchronized to allow patterned exposures and metallic structures to be written in the sample.

Microfabricated structures were imaged in situ using two-photon scanning laser microscopy (Biorad MRC-1024 scanner/controller).

TEM was performed using an Hitachi 8100S, samples were cast on Si_3N_4 grids purchased from SPI, West Chester, PA, USA.

SEM was performed on an Hitachi S-2460N; samples on a glass substrate were coated with an Au/Ir alloy by sputtering, while samples on an indium tin oxide (ITO) coated substrate were imaged without any further processing.

Enthalpies of de-interdigitation were calculated by integrating the transition peak [21,22] in the differential scanning calorimetry (DSC) plot. DSC was performed using a Shimadzu DSC 50 connected to a personal computer via a Shimadzu TA 50 thermal analyzer.

Received: August 20, 2001
Final version: November 6, 2001

[1] Y. N. Xia, E. Kim, X. M. Zhao, J. A. Rogers, M. Prentiss, G. M. Whitesides, *Science* **1996**, *273*, 347.
[2] S. R. Quake, A. Scherer, *Science* **2000**, *290*, 1536.
[3] S. M. Sze, *Semiconductor Sensors*, Wiley, New York **1994**.
[4] N. C. MacDonald, *Microelectron. Eng.* **1996**, *32*, 49.
[5] H. G. Craighead, *Science* **2000**, *290*, 1532.
[6] A. C. Templeton, M. P. Wuelfing, R. W. Murray, *Acc. Chem. Res.* **2000**, *33*, 27.
[7] T. A. Taton, R. C. Mucic, C. A. Mirkin, R. L. Letsinger, *J. Am. Chem. Soc.* **2000**, *122*, 6305.
[8] A. P. Alivisatos, K. P. Johnsson, X. G. Peng, T. E. Wilson, C. J. Loweth, M. P. Bruchez, P. G. Schultz, *Nature* **1996**, *382*, 609.
[9] M. T. Reetz, M. Winter, G. Dumpich, J. Lohau, S. Friedrichowski, *J. Am. Chem. Soc.* **1997**, *119*, 4539.
[10] M. J. Hampden-Smith, T. T. Kodas, *Chem. Vap. Deposition* **1995**, *1*, 8.
[11] P. W. Wu, W. Cheng, I. B. Martini, B. Dunn, B. J. Schwartz, E. Yablonovitch, *Adv. Mater.* **2000**, *12*, 1438.
[12] T. Deng, F. Arias, R. F. Ismagilov, P. J. A. Kenis, G. M. Whitesides, *Anal. Chem.* **2000**, *72*, 645.
[13] W. P. Wuelfing, F. P. Zamborini, A. C. Templeton, X. G. Wen, H. Yoon, R. W. Murray, *Chem. Mater.* **2001**, *13*, 87.
[14] E. Braun, Y. Eichen, U. Sivan, G. Ben-Yoseph, *Nature* **1998**, *391*, 775.
[15] J. F. Hamilton, *Adv. Phys.* **1988**, *37*, 359.
[16] M. Albota, D. Beljonne, J. L. Brédas, J. E. Ehrlich, J. Y. Fu, A. A. Heikal, S. E. Hess, T. Kogej, M. D. Levin, S. R. Marder, D. McCord-Maughon, J. W. Perry, H. Röckel, M. Rumi, C. Subramaniam, W. W. Webb, X. L. Wu, C. Xu, *Science* **1998**, *281*, 1653.
[17] C. Xu, W. W. Webb, *J. Opt. Soc. Am. B—Opt. Phys.* **1996**, *13*, 481.
[18] M. B. Mohamed, Z. L. Wang, M. A. El-Sayed, *J. Phys. Chem. A* **1999**, *103*, 10 255.
[19] R. H. Terrill, T. A. Postlethwaite, C. H. Chen, C. D. Poon, A. Terzis, A. D. Chen, J. E. Hutchison, M. R. Clark, G. Wignall, J. D. Londono, R. Superfine, M. Falvo, C. S. Johnson, E. T. Samulski, R. W. Murray, *J. Am. Chem. Soc.* **1995**, *117*, 12 537.
[20] W. Caseri, *Macromol. Rapid Commun.* **2000**, *21*, 705.
[21] A. Badia, S. Singh, L. Demers, L. Cuccia, G. R. Brown, R. B. Lennox, *Chem. Eur. J.* **1996**, *2*, 359.
[22] N. Sandhyarani, T. Pradeep, J. Chakrabarti, M. Yousuf, H. K. Sahu, *Phys. Rev. B* **2000**, *62*, R739.
[23] W. Denk, J. H. Strickler, W. W. Webb, *Science* **1990**, *248*, 73.
[24] B. H. Cumpston, S. P. Ananthavel, S. Barlow, D. L. Dyer, J. E. Ehrlich, L. L. Erskine, A. A. Heikal, S. M. Kuebler, I. Y. S. Lee, D. McCord-Maughon, J. Q. Qin, H. Röckel, M. Rumi, X. L. Wu, S. R. Marder, J. W. Perry, *Nature* **1999**, *398*, 51.
[25] S. Maruo, O. Nakamura, S. Kawata, *Opt. Lett.* **1997**, *22*, 132.
[26] K. E. Gonsalves, L. Merhari, H. P. Wu, Y. Q. Hu, *Adv. Mater.* **2001**, *13*, 703.
[27] S. Y. Kang, K. Kim, *Langmuir* **1998**, *14*, 226.
[28] R. S. Ingram, M. J. Hostetler, R. W. Murray, *J. Am. Chem. Soc.* **1997**, *119*, 9175.
[29] There is also a weak band at ~580 nm, which may be due to a charge-transfer complex or a small amount of nanoparticle clusters formed prior to laser irradiation. Given the weakness of this band and the laser wavelengths used (488 and 514.5 nm) for one-photon excitation, we believe that the band does not play a significant role in the experiments described here relative to the much stronger absorption due to the dye band. This is supported by the observation that the relative metal growth rate scales with the absorption due to the dye, for excitation at 488 and 514.5 nm. Similarly, this band should play no significant role in two-photon experiments that were done at wavelengths from 730 to 800 nm, which are far from two-photon resonance with the weak band.
[30] M. V. U. Kreibig, *Optical Properties of Metal Clusters*, Vol. 25 (Eds: R. M. O. J. U. Gonser, M. B. Pansh, H. Sakaki), Springer, New York **1995**.

Scaffolding of Polymers by Supramolecular Nanoribbons

By *Eugene R. Zubarev*, *Martin U. Pralle*, *Eli D. Sone*, and *Samuel I. Stupp**

The quest for designed structures that offer sophisticated properties to materials is one of the goals of organic materials science. Examples of such systems include chemically defined surfaces,[1] designed patterns,[2] new materials based on supramolecular structures,[3] artificial proteins,[4] and synthetic molecules that imitate protein folding.[5] A less known area is the use of self-assembly to modify polymers using supramolecular strategy. Here we report that exceedingly small amounts of self-assembling block molecules containing dendritic, rodlike,

[*] Prof. S. I. Stupp, Dr. E. R. Zubarev, Dr. M. U. Pralle, E. D. Sone
Department of Materials Science and Engineering
Department of Chemistry, and Medical School
Northwestern University
Evanston, IL 60208 (USA)
E-mail: s-stupp@northwestern.edu

  0935-9648/02/0302-0198 $ 17.50+.50/0